JACS
JOURNAL OF THE AMERICAN CHEMICAL SOCIETY
Communication
pubs.acs.org/JACS

Surface Plasmon-Driven Water Reduction: Gold Nanoparticle Size Matters

Kun Qian,[†] Brendan C. Sweeny,[†] Aaron C. Johnston-Peck,[‡] Wenxin Niu,[†] Jeremy O. Graham,[†] Joseph S. DuChene,[†] Jingjing Qiu,[†] Yi-Chung Wang,[†] Mark H. Engelhard,[§] Dong Su,[‡] Eric A. Stach,[‡] and Wei David Wei*,[†]

[†]Department of Chemistry and Center for Nanostructured Electronic Materials, University of Florida, Gainesville, Florida 32611, United States

[‡]Center for Functional Nanomaterials, Brookhaven National Laboratory, Upton, New York 11973, United States

[§]Environmental Molecular Sciences Laboratory, Pacific Northwest National Laboratory, Richland, Washington 99354, United States

Supporting Information

ABSTRACT: Water reduction under two different visible-light ranges ($\lambda > 400$ nm and $\lambda > 435$ nm) was investigated in gold-loaded titanium dioxide (Au-TiO_2) heterostructures with different sizes of Au nanoparticles (NPs). Our study clearly demonstrates the essential role played by Au NP size in plasmon-driven H_2O reduction and reveals two distinct mechanisms to clarify visible-light photocatalytic activity under different excitation conditions. The size of the Au NP governs the efficiency of plasmon-mediated electron transfer and plays a critical role in determining the reduction potentials of the electrons transferred to the TiO_2 conduction band. Our discovery provides a facile method of manipulating photocatalytic activity simply by varying the Au NP size and is expected to greatly facilitate the design of suitable plasmonic photocatalysts for solar-to-fuel energy conversion.

Photocatalytic production of H_2 from renewable sources such as H_2O and sunlight represents a promising solution to growing demands for clean and sustainable energy.[1] Recently it was discovered that the addition of plasmonic metal nanoparticles (NPs) into a semiconductor can greatly increase its photocatalytic activity for H_2O reduction, with concomitant reaction rate enhancement directly related to the localized surface plasmon resonance (SPR) of the metal NPs.[2] However, despite these exciting results, there is still no clear understanding of the exact mechanisms responsible for SPR-enhanced photocatalysis.[2a,b,i,k,m,n,p] For instance, it has been reported that Janus Au-TiO_2 photocatalysts with 70 nm Au NPs outperform those with 30 nm Au NPs for visible-light H_2 generation. This observation was attributed to the enhanced optical absorption of TiO_2 itself caused by the strong SPR-enhanced electromagnetic (EM) fields of the nearby Au NPs, leading to enhanced electron−hole (e−h) generation within the TiO_2.[2i] Meanwhile, others have shown that Au-TiO_2 with 1.87 nm Au NPs demonstrates the best activity for H_2O reduction, and it was claimed that the photoinjection of electrons from Au to TiO_2 plays a key role in the photocatalytic enhancement.[2b] Obviously, such a controversial understanding of the role of plasmonic metals, especially the impact of Au NP size on SPR-enhanced photocatalysis, impedes the development of new photocatalytic materials for efficient visible-light-driven H_2O reduction to produce H_2.

In this work, we designed a series of Au-TiO_2 heterostructures with varying Au NP sizes and evaluated their activities in visible-light-driven H_2O reduction to elucidate the specific role of the size of the Au NPs in photocatalysis. Two different mechanisms were identified in the photoreduction of H_2O under $\lambda > 400$ nm and $\lambda > 435$ nm excitations. Our study clearly shows that the previously reported high photocatalytic activity of Au-TiO_2 under $\lambda > 400$ nm excitation is actually due to direct interband excitation of the TiO_2 support itself, followed by the transfer of photoexcited electrons from TiO_2 to the supported Au NPs. However, under $\lambda > 435$ nm irradiation, the photocatalytic reduction of H_2O is dominated by SPR-mediated electron transfer (ET) from Au NPs to TiO_2. Furthermore, we have conclusively demonstrated that Au NP size is essential for controlling the reduction potentials of the transferred electrons in the conduction band (CB) of TiO_2. This approach provides a facile way to manipulate the photocatalytic activity of Au-TiO_2 heterostructures by simply varying the size of the Au NPs. Our discovery represents a potentially universal strategy for the construction of new types of plasmonic-metal/semiconductor heterostructures as valuable photocatalysts for solar-to-fuel energy conversion.

In our experiments, Au-TiO_2 heterostructures with different Au NP sizes were fabricated using deposition−precipitation (DP)[3] and photodeposition (PD)[4] methods onto P25 (Degussa) TiO_2 [see the Supporting Information (SI)]. Figure 1 shows medium-angle annular dark-field scanning transmission electron microscopy (MAADF-STEM) and high-resolution (HR) STEM images of the Au-P25 nanostructures. The average size of the Au NPs was 4.4 ± 1.7 nm (Figure S1 in the SI) for 5% Au-P25-DP (defined as "small Au-P25"; Figure 1A,C). The 5% Au-P25-PD yielded large Au NPs with an average size of 67 ± 17 nm (defined as "large Au-P25"; Figures 1B,D and S1). The Au-P25 heterostructures fabricated using both methods exhibited direct physical contact at the metal−semiconductor interface (Figure 1C,D and S2). Additional X-ray photoelectron spectroscopy

Received: April 24, 2014
Published: June 27, 2014

   dx.doi.org/10.1021/ja504097v | J. Am. Chem. Soc. 2014, 136, 9842−9845

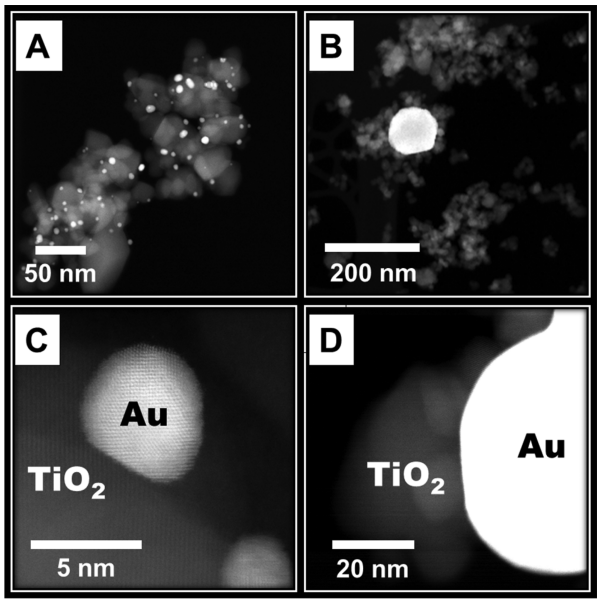

Figure 1. (A, B) STEM images of (A) small and (B) large Au-P25. (C, D) HR-STEM images showing the Au−TiO_2 interface for (C) small and (D) large Au-P25.

(XPS) results confirmed that the deposited Au NPs were metallic Au(0) in both the small Au-P25 and large Au-P25 heterostructures (Figure S3).

Following the method outlined in previous literature,[2b,f] the activities of the prepared Au-P25 photocatalysts were tested for H_2O reduction under two different visible-light conditions. As shown in Figure 2A and Table S1 in the SI, under $\lambda > 400$ nm

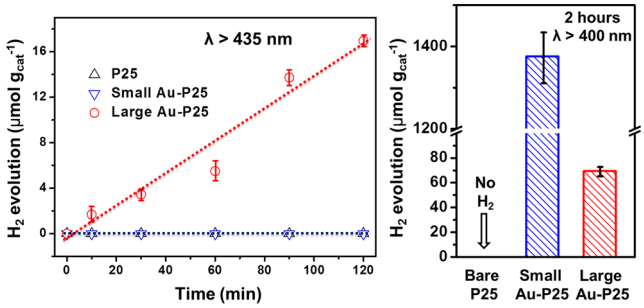

Figure 2. H_2O reduction activities of Au-P25 photocatalysts under (A) $\lambda > 400$ nm and (B) $\lambda > 435$ nm irradiation.

excitation, the amount of H_2 production in 2 h for small Au-P25 (1376 ± 60 μmol_{H_2} g_{cat}^{-1}) was ca. 20 times higher than that for large Au-P25 (69.4 ± 3.5 μmol_{H_2} g_{cat}^{-1}), consistent with previous reports that Au-TiO_2 heterostructures with smaller Au NPs exhibit better activity.[2b,h,i,5] However, this observation seems counterintuitive to the often-claimed SPR-induced photoinjection of electrons from Au to the TiO_2 support,[2b] since the smaller Au NPs exhibit weaker SPR intensity (Figure S4). Furthermore, if the SPR-induced photoinjection mechanism were operative in these photocatalysts, one would expect them to exhibit similar differences under $\lambda > 435$ nm excitation. However, to our surprise, no H_2 production was detected over small Au-P25, while large Au-P25 still produced a significant amount of H_2 (16.9 ± 0.9 μmol_{H_2} g_{cat}^{-1}) under identical experimental conditions (Figure 2B). These results strongly suggest that the enhanced photocatalytic activities of Au-P25 under $\lambda > 400$ nm irradiation are not due to the Au SPR.

It is very likely that the observed photocatalytic activity enhancement for Au-P25 under $\lambda > 400$ nm light is attributable to a mechanism similar to the well-known ultraviolet (UV) light-mediated ET mechanism.[6] It is noted that the UV−vis spectrum of P25 always shows a slight "tail" beyond 400 nm (Figure S5).[2n,q,6a] Although no H_2 production was detected over bare P25 under $\lambda > 400$ nm light (Figure 2A and Table S1), this is probably due to the rapid recombination of e−h pairs generated through direct excitation of TiO_2. Once Au NPs are incorporated into P25 to form Au-P25 heterostructures, the Au NPs can facilitate charge separation at the Au−TiO_2 interface and promote the transfer of photoexcited electrons from the TiO_2 CB to the Au NPs, inhibiting the e−h pair recombination process. Since smaller Au NPs induce a greater negative shift in the Fermi level and better charge separation than large Au NPs,[7] a higher photocatalytic activity for H_2O reduction in the small Au-P25 photocatalysts is expected. Significantly, photoluminescence (PL) studies of the Au-P25 photocatalyst support this mechanism. Small Au-P25 exhibits the lowest TiO_2 PL intensity (10445 ± 99) (Figure S6). This "quenched" PL is due to the transfer of the excited electrons from the TiO_2 CB to the attached Au NPs, providing direct evidence of better charge separation with the smaller Au NPs under $\lambda > 400$ nm excitation.[8] It is worth noting that many previous studies of Au-TiO_2 photocatalysis ignored the absorption edge of TiO_2 beyond 400 nm and attributed the enhanced photocatalytic activity to the metal SPR. Our results conclusively show that full consideration of possible visible-light-mediated ET from TiO_2 to Au NPs is necessary under such circumstances.

The significant photocatalytic activity observed for H_2O reduction with large Au-P25 under $\lambda > 435$ nm irradiation should be attributed to the Au SPR. Since no H_2 production was detected over small Au-P25 under $\lambda > 435$ nm excitation (Figure 2B), this result strongly indicates that the extended tail beyond 435 nm in the P25 extinction spectrum (Figure S5) is attributable to photon scattering rather than direct light absorption. Such an observation leads us to conclude that the aforementioned mechanism of visible-light-mediated ($\lambda > 400$ nm) ET from TiO_2 to Au NPs does not apply for this system. Therefore, the photoinduced catalytic activity must originate from the intrinsic optical properties of the supported Au NPs, as the large Au-P25 photocatalysts exhibit a broad feature between 500 and 700 nm indicative of the Au SPR (Figure S4). Further investigation of the photocatalytic activity for water reduction under $\lambda > 435$ nm light shows an approximately first-order dependence on the incident light power (Figure S7), confirming that this process is driven by visible-light excitation of the Au NPs.[9]

It is known that SPR excitation of Au NPs can influence the photocatalytic activity through four potential mechanisms: (1) local photothermal heating,[10] (2) enhanced EM fields,[2d,i,6b,11] (3) resonant photon scattering,[2d] and (4) SPR-mediated ET from Au NPs to the support.[2a,12] However, the low power of our light source (1.0 W/cm^2) was unable to heat the system enough to directly split H_2O,[2a,b,i] as further confirmed by the modest increase in solution temperature (from 25 to 35 °C) measured during the 2 h irradiation period. Furthermore, no direct interband transitions occurred within the P25 under $\lambda > 435$ nm irradiation (Figure 2B), so the SPR-enhanced EM fields and resonant photon scattering can also be excluded as possible mechanisms for the generation of e−h pairs within P25. The observed H_2 production from large Au-P25 under $\lambda > 435$ nm

dx.doi.org/10.1021/ja504097v | J. Am. Chem. Soc. 2014, 136, 9842−9845

irradiation can thus only be attributed to SPR-mediated ET from the Au NPs to the TiO_2 support. It is known that a Schottky barrier (ϕ) is formed at the Au−TiO_2 interface when Au NPs make direct physical contact with TiO_2.[13] Upon excitation of the Au SPR with $\lambda > 435$ nm, intense SPR-enhanced EM fields are generated on the Au NP surface, significantly increasing the yield of interfacial "hot electrons" with a higher potential energy (E_{SPR}) than ϕ at the interface. According to Marcus theory,[14] the large potential energy difference ($E_{SPR} - \phi$) will induce fast and efficient transfer of "hot electrons" to the CB of P25. The Schottky barrier at the interface also helps the transferred "hot" electrons accumulate in the TiO_2 CB, preventing them from traveling back to the Au NPs. Since no holes are generated in the valence band (VB) of TiO_2 under $\lambda > 435$ nm excitation, the transferred "hot electrons" in the TiO_2 CB should have much longer lifetimes,[2r] fostering the reduction of H_2O to produce H_2.

The photodeposition of Pt NPs on the Au-P25 photocatalysts under $\lambda > 435$ nm irradiation further reinforces the SPR-mediated ET mechanism and elucidates the specific role of the Au SPR in the enhanced photocatalytic activity. Figure S8 shows that 1.8 ± 0.5 nm Pt NPs were detected on the TiO_2 surface of the large Au-P25 photocatalyst after 2 h of irradiation, verifying that the Au SPR can facilitate ET from Au NPs to the TiO_2 surface, where $PtCl_6^{2-}$ ions are reduced by the transferred "hot" electrons to form Pt NPs.

Interestingly, 1.5 ± 0.6 nm Pt NPs were also detected on the TiO_2 surface of small Au-P25 after 2 h of irradiation (Figure S9), suggesting that SPR-mediated ET also occurs in the photocatalysts with smaller Au NPs. In fact, as shown in previous UV−vis spectra (Figure S4), although the SPR intensity is much weaker than that of the 67 nm Au NPs, the 4.4 nm Au NPs do exhibit SPR features that could facilitate ET to TiO_2. However, compared with large Au-P25, no H_2 production was detected for small Au-P25 under identical experimental conditions, indicating that the chemical reduction potentials of the transferred electrons must be different in these two photocatalysts.

As described previously, the Schottky barrier at the Au−TiO_2 interface functions as a barrier for the transferred electrons, preventing these "hot electrons" from returning to the Au NPs and leading to an accumulation of these transferred electrons in the TiO_2 CB. More importantly, such accumulation allows the transferred electrons to achieve higher energy levels in the TiO_2 CB and increases their reduction potentials. The energy levels reached by the transferred electrons in the TiO_2 CB are determined by the ET efficiencies, which are directly correlated with the Au SPR intensities. It is known that the reduction potential of $PtCl_6^{2-}$ (~ +0.3 V vs NHE at pH 7) is much lower than the TiO_2 CB minimum (Scheme 1). Thus, the Pt precursor

Scheme 1. Proposed Mechanism for Manipulating SPR-Mediated ET for Photocatalysis by Controlling Au NP Size

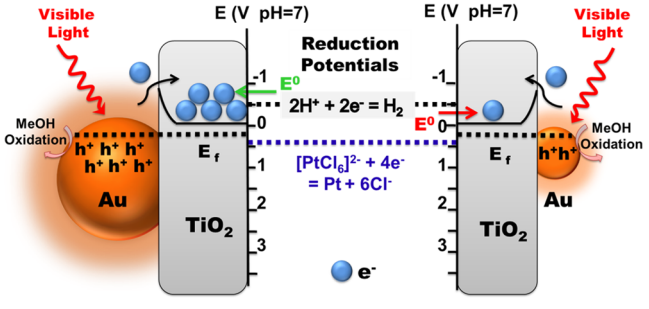

can easily be reduced by the transferred electrons within both small Au-P25 and large Au-P25. However, the H_2 evolution potential is known to be close to the CB of TiO_2,[2d,15] making H_2O reduction a good benchmark for inspecting the subtle energy difference between the transferred "hot electrons" of these two Au-P25 photocatalysts. For small Au-P25, the weaker SPR intensity of the 4.4 nm Au NPs leads to a low ET efficiency, and the buildup of transferred electrons is insufficient to bring them to an energy level higher than the H_2 evolution potential (Scheme 1, right). Meanwhile, the 67 nm Au NPs in large Au-P25 produce a more intense SPR that greatly facilitates the transfer of electrons to the TiO_2 CB, where their accumulation makes those transferred electrons "hot" enough to overcome the overpotential required for H_2O reduction (Scheme 1, left).

This discovery also suggests that varying the Au NP size should enable fine manipulation of the reduction potentials of the transferred electrons, thereby modifying the photocatalytic activity. To demonstrate this, we purposely deposited 4% equivalence of Au to the 1% Au-P25-DP using the PD method (defined as "1% Au-P25-DP−4% Au-PD"). It was observed that the average particle size increased from 4.4 ± 1.1 nm to 37 ± 8.1 nm (Figure S10). As expected, 1% Au-P25-DP−4% Au-PD showed photoactivity similar to that of large Au-P25 and produced a significant amount of H_2 (4.7 ± 0.3 $\mu mol_{H_2}\ g_{cat}^{-1}$) under $\lambda > 435$ nm irradiation (Figure 3). The reduced amount of

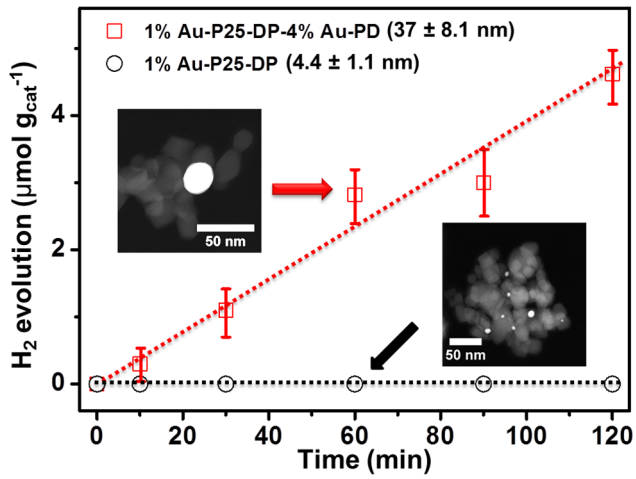

Figure 3. H_2O reduction activities over 1% Au-P25-DP and 1% Au-P25-DP−4% Au-PD photocatalysts under $\lambda > 435$ nm irradiation.

H_2 production relative to that observed for large Au-P25 (67 nm Au NPs) further suggests that the size of the Au NPs plays an essential role in efficient H_2O reduction under visible-light irradiation. To our knowledge, these results are the first to unambiguously clarify the critical role of plasmonic-metal NP size in determining the SPR-mediated ET efficiency and the correlated reaction activities for plasmon-driven photocatalysis. These insights should provide a foundation for developing novel strategies to control and tune the reduction potential of transferred electrons for specific engineering of reaction pathways in multistep reduction processes with subtle differences in their reduction potentials, such as the photoconversion of CO_2 into CH_4.[15a]

In summary, we have successfully differentiated two different mechanisms involved in the photoreduction of H_2O under $\lambda > 400$ nm and $\lambda > 435$ nm excitations. Previous ambiguity concerning the high photocatalytic activity of Au-TiO_2 systems

dx.doi.org/10.1021/ja504097v | J. Am. Chem. Soc. 2014, 136, 9842−9845

with smaller Au NPs under $\lambda > 400$ nm irradiation has been clarified, with the enhanced activity attributed to direct interband excitation within TiO_2 and subsequent ET from TiO_2 to Au NPs. Our study demonstrates that the Au SPR is vital for visible-light-driven H_2O reduction under $\lambda > 435$ nm light. More specifically, we have discovered that control of the Au NP size is essential for efficient SPR-mediated ET and plays a critical role in determining the reduction potential of the transferred electrons in the TiO_2 CB. We have further shown that the reduction potential of the transferred electrons can be easily tuned by varying Au NP size, providing a simple means of tailoring their photocatalytic activity. Such a strategy should be applicable to other plasmonic-metal/semiconductor photocatalysts and is expected to facilitate the design of advanced plasmonic photocatalysts for efficient solar-to-fuel energy conversion.

■ ASSOCIATED CONTENT

Supporting Information

Experimental procedures and supporting data. This material is available free of charge via the Internet at http://pubs.acs.org.

■ AUTHOR INFORMATION

Corresponding Author

wei@chem.ufl.edu

Notes

The authors declare no competing financial interest.

■ ACKNOWLEDGMENTS

We thank NSF for support under Grant CHE-1308644 and the CCI Center for Nanostructured Electronic Materials (CHE-1038015). EM work was carried out in part at the Center for Functional Nanomaterials at Brookhaven National Laboratory through User Proposal BNL-CFN-31913, supported by the U.S. Department of Energy, Office of Basic Energy Sciences under Contract DE-AC02-98CH10886. A portion of the research was performed using EMSL (User Proposal 40065), a National Scientific User Facility sponsored by the Department of Energy's Office of Biological and Environmental Research located at Pacific Northwest National Laboratory.

■ REFERENCES

(1) (a) Fujishima, A.; Honda, K. *Nature* **1972**, *238*, 37. (b) Asahi, R.; Morikawa, T.; Ohwaki, T.; Aoki, K.; Taga, Y. *Science* **2001**, *293*, 269. (c) Mayer, M. T.; Lin, Y. J.; Yuan, G. B.; Wang, D. W. *Acc. Chem. Res.* **2013**, *46*, 1558. (d) Lee, C.; Aikens, C. M. *J. Phys. Chem. A* **2014**, *118*, 598.

(2) (a) Bian, Z. F.; Tachikawa, T.; Zhang, P.; Fujitsuka, M.; Majima, T. *J. Am. Chem. Soc.* **2014**, *136*, 458. (b) Silva, C. G.; Juárez, R.; Marino, T.; Molinari, R.; García, H. *J. Am. Chem. Soc.* **2011**, *133*, 595. (c) Gao, H. W.; Liu, C.; Jeong, H. E.; Yang, P. D. *ACS Nano* **2012**, *6*, 234. (d) Linic, S.; Christopher, P.; Ingram, D. B. *Nat. Mater.* **2011**, *10*, 911. (e) Thimsen, E.; Le Formal, F.; Grätzel, M.; Warren, S. C. *Nano Lett.* **2011**, *11*, 35. (f) Primo, A.; Marino, T.; Corma, A.; Molinari, R.; García, H. *J. Am. Chem. Soc.* **2011**, *133*, 6930. (g) Primo, A.; Corma, A.; García, H. *Phys. Chem. Chem. Phys.* **2011**, *13*, 886. (h) Priebe, J. B.; Karnahl, M.; Junge, H.; Beller, M.; Hollmann, D.; Brückner, A. *Angew. Chem., Int. Ed.* **2013**, *52*, 11420. (i) Seh, Z. W.; Liu, S. H.; Low, M.; Zhang, S. Y.; Liu, Z. L.; Mlayah, A.; Han, M. Y. *Adv. Mater.* **2012**, *24*, 2310. (j) Zhang, X. M.; Chen, Y. L.; Liu, R. S.; Tsai, D. P. *Rep. Prog. Phys.* **2013**, *76*, 046401. (k) Tanaka, A.; Hashimoto, K.; Kominami, H. *J. Am. Chem. Soc.* **2014**, *136*, 586. (l) Fuku, K.; Hayashi, R.; Takakura, S.; Kamegawa, T.; Mori, K.; Yamashita, H. *Angew. Chem., Int. Ed.* **2013**, *52*, 7446. (m) Wang, F.; Li, C. H.; Chen, H. J.; Jiang, R. B.; Sun, L. D.; Li, Q.; Wang, J. F.; Yu, J. C.; Yan, C. H. *J. Am. Chem. Soc.* **2013**, *135*, 5588. (n) Yan, J. Q.; Wu, G. J.; Guan, N. J.; Li, L. D. *Chem. Commun.* **2013**, *49*, 11767. (o) Qian, H. F.; Zhu, M. Z.; Wu, Z. K.; Jin, R. C. *Acc. Chem. Res.* **2012**, *45*, 1470. (p) Sastre, F.; Oteri, M.; Corma, A.; García, H. *Energy Environ. Sci.* **2013**, *6*, 2211. (q) Warren, S. C.; Thimsen, E. *Energy Environ. Sci.* **2012**, *5*, 5133. (r) DuChene, J. S.; Sweeny, B. C.; Johnston-Peck, A. C.; Su, D.; Stach, E. A.; Wei, W. D. *Angew. Chem., Int. Ed.* **2014**, DOI: 10.1002/anie.201404259.

(3) (a) Qian, K.; Luo, L. F.; Bao, H. Z.; Hua, Q.; Jiang, Z. Q.; Huang, W. X. *Catal. Sci. Technol.* **2013**, *3*, 679. (b) Qian, K.; Huang, W. X.; Jiang, Z. Q.; Sun, H. X. *J. Catal.* **2007**, *248*, 137.

(4) Tanaka, A.; Hashimoto, K.; Kominami, H. *J. Am. Chem. Soc.* **2012**, *134*, 14526.

(5) Awate, S. V.; Deshpande, S. S.; Rakesh, K.; Dhanasekaran, P.; Gupta, N. M. *Phys. Chem. Chem. Phys.* **2011**, *13*, 11329.

(6) (a) Murdoch, M.; Waterhouse, G. I. N.; Nadeem, M. A.; Metson, J. B.; Keane, M. A.; Howe, R. F.; Llorca, J.; Idriss, H. *Nat. Chem.* **2011**, *3*, 489. (b) Pu, Y. C.; Wang, G. M.; Chang, K. D.; Ling, Y. C.; Lin, Y. K.; Fitzmorris, B. C.; Liu, C. M.; Lu, X. H.; Tong, Y. X.; Zhang, J. Z.; Hsu, Y. J.; Li, Y. *Nano Lett.* **2013**, *13*, 3817.

(7) (a) Subramanian, V.; Wolf, E. E.; Kamat, P. V. *J. Am. Chem. Soc.* **2004**, *126*, 4943. (b) Sabio, E. M.; Chamousis, R. L.; Browning, N. D.; Osterloh, F. E. *J. Phys. Chem. C* **2012**, *116*, 3161.

(8) Stevanovic, A.; Büttner, M.; Zhang, Z.; Yates, J. T., Jr. *J. Am. Chem. Soc.* **2012**, *134*, 324.

(9) (a) Ingram, D. B.; Linic, S. *J. Am. Chem. Soc.* **2011**, *133*, 5202. (b) Linic, S.; Christopher, P.; Xin, H. L.; Marimuthu, A. *Acc. Chem. Res.* **2013**, *46*, 1890.

(10) Qiu, J. J.; Wu, Y. C.; Wang, Y. C.; Engelhard, M. H.; McElwee-White, L.; Wei, W. D. *J. Am. Chem. Soc.* **2013**, *135*, 38.

(11) (a) Bukasov, R.; Ali, T. A.; Nordlander, P.; Shumaker-Parry, J. S. *ACS Nano* **2010**, *4*, 6639. (b) Carim, A. I.; Gu, J. S.; Maldonado, S. *ACS Nano* **2011**, *5*, 1818. (c) Wei, W.; Li, S. Z.; Qin, L. D.; Xue, C.; Millstone, J. E.; Xu, X. Y.; Schatz, G. C.; Mirkin, C. A. *Nano Lett.* **2008**, *8*, 3446. (d) Wei, W.; Li, S. Z.; Millstone, J. E.; Banholzer, M. J.; Chen, X. D.; Xu, X. Y.; Schatz, G. C.; Mirkin, C. A. *Angew. Chem., Int. Ed.* **2009**, *48*, 4210.

(12) (a) Mubeen, S.; Lee, J.; Singh, N.; Krämer, S.; Stucky, G. D.; Moskovits, M. *Nat. Nanotechnol.* **2013**, *8*, 247. (b) Knight, M. W.; Sobhani, H.; Nordlander, P.; Halas, N. J. *Science* **2011**, *332*, 702.

(13) Lee, Y. K.; Jung, C. H.; Park, J.; Seo, H.; Somorjai, G. A.; Park, J. Y. *Nano Lett.* **2011**, *11*, 4251.

(14) Huss, A. S.; Bierbaum, A.; Chitta, R.; Ceckanowicz, D. J.; Mann, K. R.; Gladfelter, W. L.; Blank, D. A. *J. Am. Chem. Soc.* **2010**, *132*, 13963.

(15) (a) Inoue, T.; Fujishima, A.; Konishi, S.; Honda, K. *Nature* **1979**, *277*, 637. (b) Hagfeldt, A.; Grätzel, M. *Chem. Rev.* **1995**, *95*, 49. (c) Hoffmann, M. R.; Martin, S. T.; Choi, W. Y.; Bahnemann, D. W. *Chem. Rev.* **1995**, *95*, 69. (d) Rosseler, O.; Shankar, M. V.; Du, M. K. L.; Schmidlin, L.; Keller, N.; Keller, V. *J. Catal.* **2010**, *269*, 179.